SAND2017-4327C

Rocket Motor Exhaust Thermal Environment Characterization

Jonathan Height[1], A. B. Donaldson[2], Walt Gill[2], Nadir Yilmaz[3, *]

[1] *Mechanical Design, Sandia National Laboratories, Albuquerque, NM 87123, U.S.A*
[2] *Fire Sciences and Technologies, Sandia National Laboratories, Albuquerque, NM 87123, U.S.A*
[3] *Department of Mechanical Engineering, New Mexico Institute of Mining and Technology, Socorro, NM 87801, U.S.A*

*Correspondence to: Nadir Yilmaz, Department of Mechanical Engineering, New Mexico Institute of Mining and Technology, Socorro, NM 87801, U.S.A.
[†]E-mail: yilmaznadir@yahoo.com , Phone: (575)835-5304, Fax: (575)835-5209

Abstract

This study experimentally examines the heat flux to objects inside and outside of a firing solid propellant rocket motor plume by measuring the heat flux to gages located at various positions from the plume. Because the application of interest may involve multiple motors firing simultaneously, the heat flux from multiple motors is projected based on data collected for a single motor test, and compared to the data for two configurations of three motor tests. Data showing the enhancement from three motors firing can be substantially higher than a single motor firing when the three motors are arranged in a triangular bundle, but this was not found to be the case when the three motors were arranged in a linear bundle (linear to the instrumentation). Based on results of this study, it was concluded that a material of concern which is exposed to as many as 14 motors firing simultaneously, should survive.

Keywords: Thermal Analysis for Solid Propellant Plumes, Rocket Motor Exhaust, Rocket Plume Heat Flux

1. Introduction

Much research effort has been devoted to understanding the thermal environment internal or external to the plume of a firing solid propellant rocket. These studies have been primarily motivated by survival of launch hardware, or to the hazard assessment for high value payloads which could sustain damage and breach. Properties such as temperature, heat flux, species composition, state of aluminum particles if included in propellant composition, and velocity, all have been of particular interest; see, for example [1,2,3,4]. The previous work has bearing on safety analysis for intentional abort, or accidental explosion of a solid propellant motor either on the launch pad, or near the ground. Recent efforts have attempted to incorporate this information into reactive computational fluid dynamics codes to project worst case scenarios to assist in the design of thermal protection systems and to quantify the hazards associated with such accidents. To date, there still remains uncertainty in the full definition of the thermal environment created by the plume of a firing rocket motor.

Outside of the propellant plume, there can be intense thermal loading to nearby objects which are within the line of sight of the plume or in proximity to the exhaust gases. Examples might include heat flux to a soldier while firing shoulder mounted rocket launchers, or to the crew and launch platform for mobile rocket launch systems.

The thermal characteristics of the rocket motor exhaust provides valuable data for the design of experiments at Sandia National Laboratories test facilities. Understanding the thermal characteristics allows engineers to ensure that the thermal environment from the exhaust does not affect surrounding test equipment or facilities. The objective of the thermal analysis is to characterize the rocket propellant exhaust plume and determine if a test fixture, in this case, a tow rope covered by high temperature insulation, will survive the plume from multiple motors

firing simultaneously. To do this, the heat flux versus distance along the plume center line of a burning rocket motor was determined for a single motor, and for two configurations of three motors. Heat flux was determined from the response of special mounted thermocouples on target coupons located along a rail that ran parallel to the plume center line. The total burn time of the rocket is ~1 second, so a sampling speed of 2500 Hz was needed to yield descriptive heat flux results.

2. Experiments

2.1. Laboratory Experiments

As a precursor to the full-scale rocket motor test, a laboratory-scale experiment was conducted to investigate the temperature rise seen the tow rope when subjected to a high heating rate. A 1-foot section of the insulation covered rope was exposed to a radiant heat cavity that delivered ~100,000 W/m^2 as step input to the system. A thermocouple on the outside of the insulation was used to establish the surface temperature from the exposure, and another thermocouple was mounted on the surface of the rope under the insulation. Figure 1 shows: a) the surface thermocouple mounted to the insulation next to the rope, b) the assembled system with the rope inside the insulation and high temperature insulation (white) to protect thermocouple leads and mount, and c) the system inserted into the radiant heat cavity.

a) b) c)

Figure 1. a) Insulation with attached thermocouple, b) assembled system and c) system in radiant heat cavity

2.2. Full-Scale Experiments

2.2.1. Thermal Instrumentation

In a test to determine the survivability of the tow rope in or near a rocket motor plume, a rail was placed parallel to the plume centerline along with the tow rope under test. The rail was designed to support thermal instrumentation and protect the signal lines from the high temperature gas flow environment. Each rail consisted of two (2) C-channels joined together by flanges, forming a square tube. Two steel plates along the top and bottom connected the two channels together. The steel plates were welded to one c-channel, and mechanically attached to the other using bolts. This allowed separation of the c-channels during installation of the thermocouples. Figure 2 shows the as-built thermal rails.

Figure 2. Thermal rails and insulated tow rope in place

Heat flux to the rail was determined from the response of special mounted thermocouples on target coupons located along the rail. Figure 3 shows the location of intrinsic and NANMAC thermocouples on each thermal rail. Figure 4 shows the metal coupons installed on the rail.

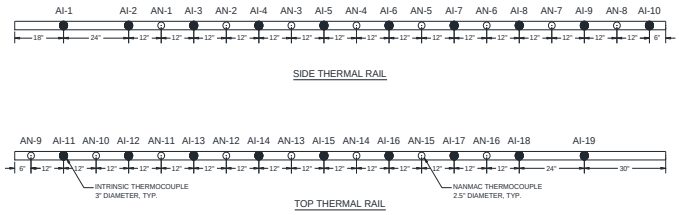

Figure 3. Thermocouple Layout

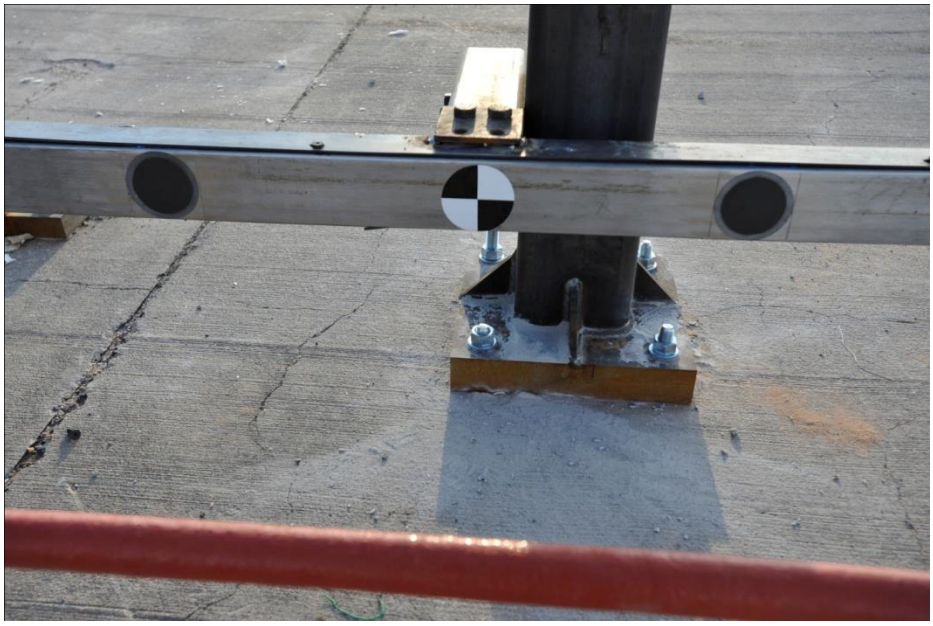

Figure 4. Installed Intrinsic Thermocouples (orange rope insulation appears in foreground)

2.2.2. Instrumentation Support Structure

The instrumentation support structure provided support for the rails at a specified distance from the centerline of the rocket motors, while resisting the thermal and flow loads created by the rocket motor exhaust. The main support structures consisted of 6”x6” x 3/8” square tubing with a 2” inch thick steel base plate anchored to concrete using four 3/4” concrete wedge anchors. The 3-1/2” x 3-1/2” x 3/16” square tubing supported the cantilevered instrumentation rails using a bolted connection. For adjustment of the cantilever with respect to the rocket motor centerline, 5/8” thru bolt holes, spaced 1” on center, on the 3-1/2” x 3-1/2” x 3/16” square tubing, were used. Figure 5 shows the as-built thermal instrumentation support structure.

Figure 5. Instrumentation Rail Support Structure and Insulated Rope

Static fire tests were captured using high-speed (HS), real-time high definition (HD), and infrared (IR) thermal cameras set up in three locations. The locations are detailed in the site layout **Error! Reference source not found.** in Figures 6 and 7.

Two tests were performed with the rails configured as shown in Figure 6, below.

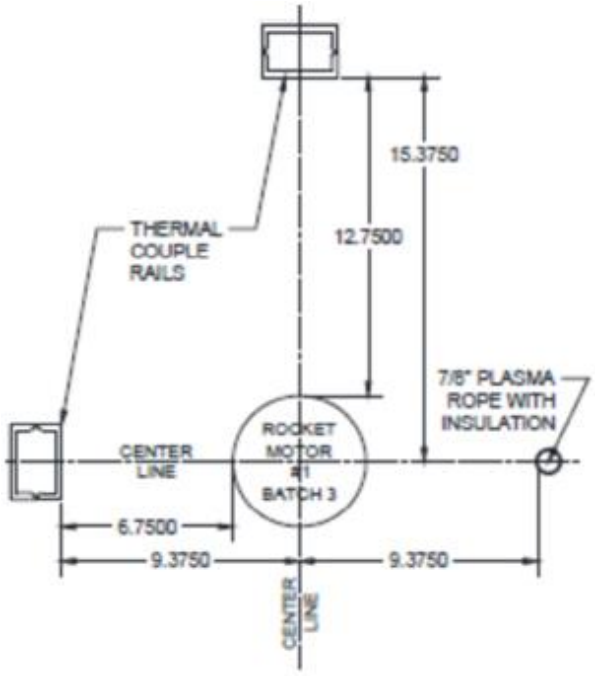

Figure 6a: Single Motor Test

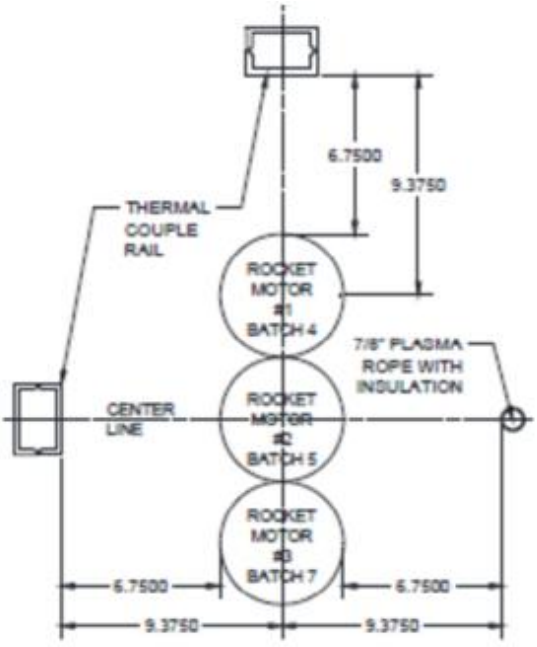

Figure 6b: Triple Motor Test

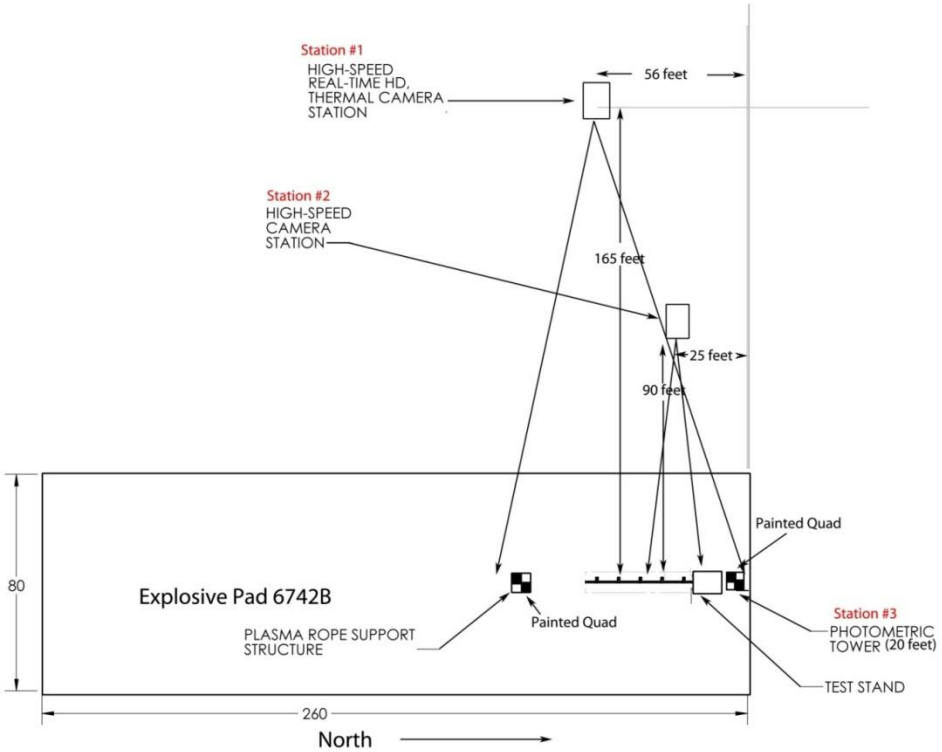

Figure 7. Camera station location diagram

All three camera stations used quadrille stadia boards positioned within each camera's field of view providing a series of spatial camera calibrations for both IR and visible data collection systems. The area imaged by the Phantom v12 camera also used quadrille targets affixed to instrumentation rails to refine the spatial calibration. All of the Phantom high-speed camera systems were synced together using IRIG-B satellite time code pulses. IRIG enabled synced camera time to the fire-set thermal and instrumentation time clocks. As a backup, a FIDU strobe unit, positioned near the rocket motors, provided an optically zero origin signal for the three camera stations. This optical FIDU assisted analysis of plume data particularly for cameras that did not include the rocket nozzle within their FOV. Figure 8 shows screen shots of a single motor test with IR and HD cameras for illustration.

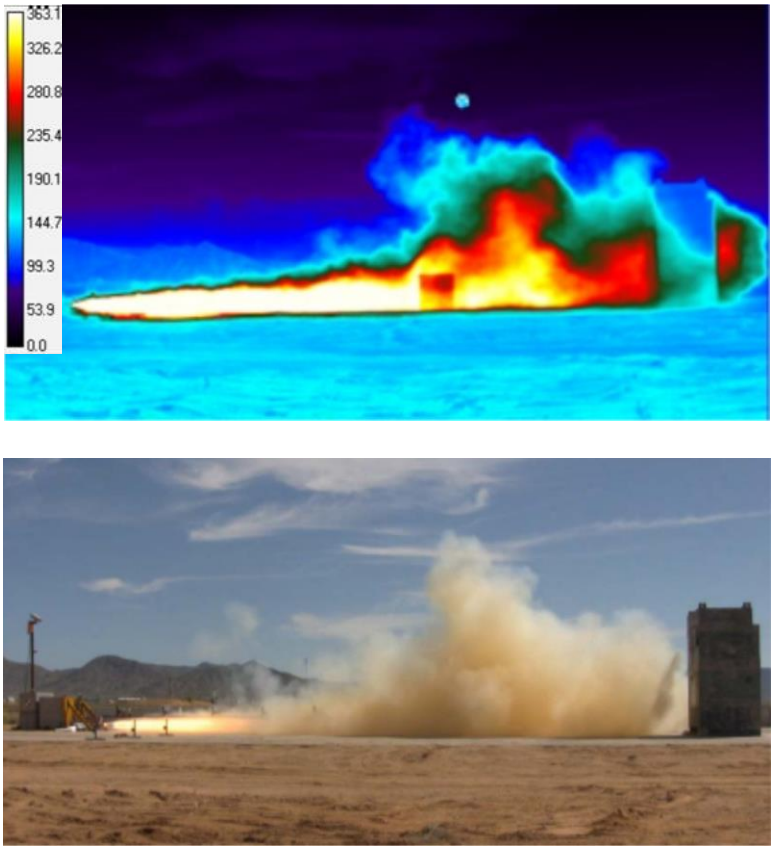

Figure 8. IR and HD Camera Screenshots of Single Motor Test

Two types of thermocouples, intrinsic and Nanmac®, were used for measurement of the heat flux during the static fire test. The NANMAC® thermocouples provide ideal millisecond response times for the high flow exhaust rates created by the rocket motors. As a cost savings, intrinsic thermocouples were also used during the test. The intrinsic thermocouples consisted of type K thermocouples tack welded to the back of 3" diameter, 0.01" thin stainless steel puck (see Figure 9). Prior to installation, the thin wall pucks were conditioned to 1000°C to pre-set the stainless steel emissivity. Upon completion of the thermocouple installation onto the puck, the pucks were welded to the thermocouple rails.

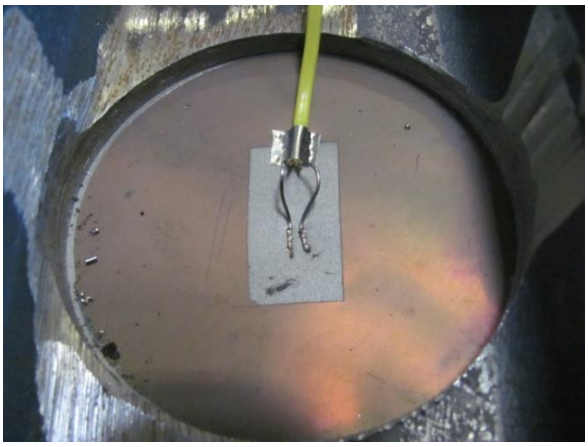

Figure 9. Intrinsic Thermocouple

The NANMAC® thermocouples used in these measurements were screwed into a 2.5" diameter, 0.5" thick stainless steel puck to simulate the semi-infinite wall condition. This thermocouple design can withstand extreme thermal conditions and provides surface temperature measurements even as the surface of the thermocouple degrades. Figure 9 shows a NANMAC® thermocouple used in this experiment.

Figure 10. NANMAC® Thermocouple

3. Results

3.1. Laboratory Tests

Figure 10 (a) shows the response of the rope thermocouple. Starting time was selected from the first rise of the outer surface thermocouple. If this is treated as a linear system, then

temperature rise of the rope surface scales with the input surface heat flux as shown in Figure 11 (b).

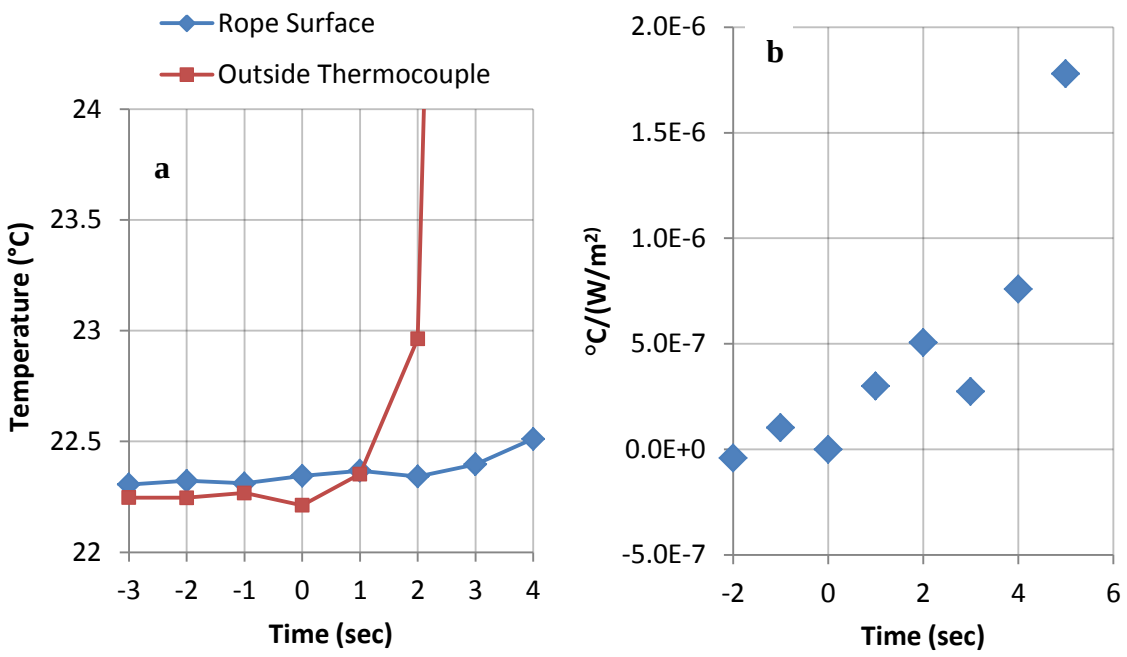

(a) **(b)**

Figure 11. (a) Temperature Response to 100,000 W/m^2 Step Input and (b) Normalized Temperature Response to Step Flux Input

After 1 second rise time, the temperature rise/flux is approximately 3x10^{-7} C/(W/m^2). Projected calculations show a flux value of 3,000,000 W/m^2 for the 14 rocket motor case with doubled flux. This gives a projected 1°C rise at the rope after one (1) second. This indicates the thermal system is more than adequate for thermally protecting the rope from the rocket plume.

It may be possible that the system is not linear. This would happen if there were a phase change in the insulation material, if the thermal conductivity were strong function of the temperature, or if radiation played a role in the heat transfer within the insulation. In such cases,

the temperature response of the rope surface could be somewhat higher. However, at the present time, it is doubtful the results from a higher step input would be significantly different.

3.2.Full-Scale Tests (Single Motor)

In the single motor test, all instrumentation (including the plasma rope) survived the plume exposure. Heat flux to the rail caused thermocouples to respond as expected. Figure 12 and Figure 13 provide sample plots for intrinsic and NANMAC® thermocouple data.

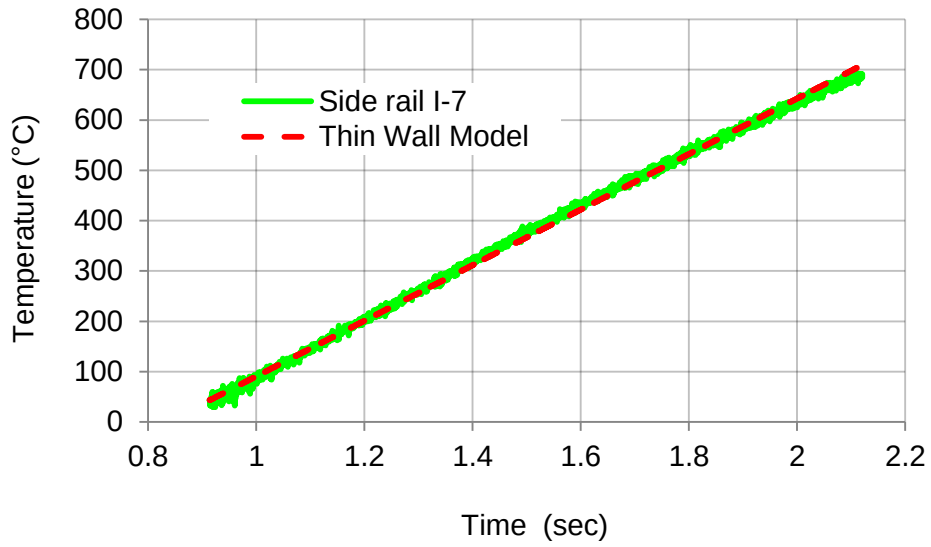

Figure 12. Sample Intrinsic Thermocouple Data and Lumped Mass Capacitance Fit

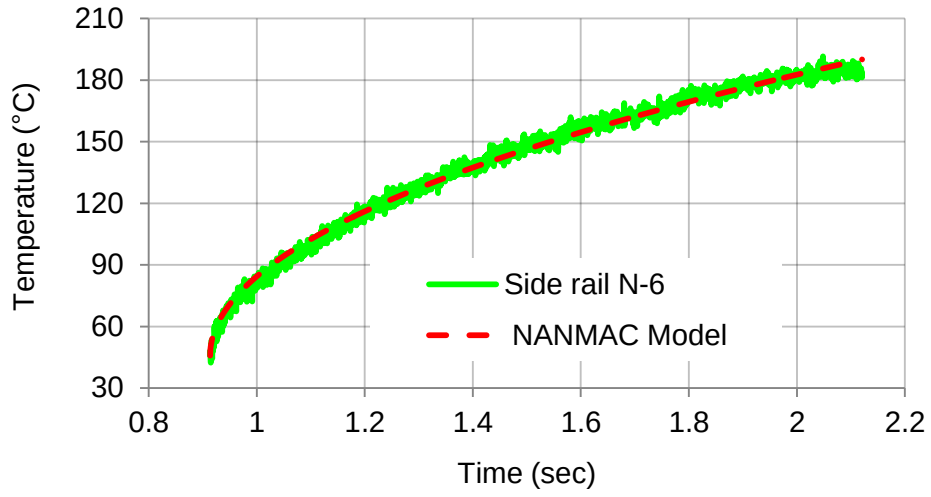

Figure 13. Sample NANMAC® Thermocouple Data and Transient Semi-Infinite Wall Fit

The data were collected for each thermocouple on both rails for both tests. From this, a best fit was found using $T \propto t$ for the lumped mass capacitance method, and $T \propto t^{1/2}$ for the semi-infinite wall model. This fit yielded a single heat flux per unit area (q) for each sensor at various locations on the rails. Figure 14 summarizes the results of these heat fluxes at various locations for the single motor test. All of these results include a 1.395 thickness multiplication factor to correct the intrinsic effective thickness. It is important to note that the top rail and side rail were measuring heat flux at different distances from the plume axis.

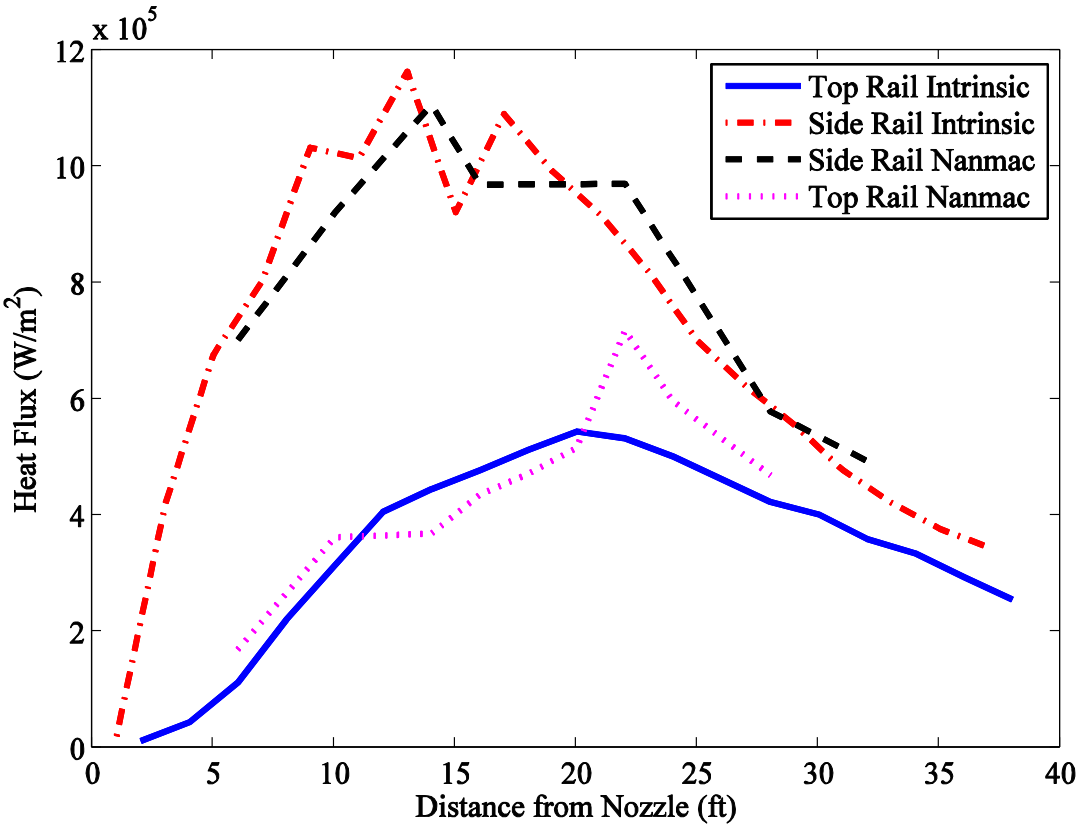

Figure 14. Single Motor Heat Flux Results with Distance from the Nozzle

3.3.Full-Scale Tests (Triple Motor arranged in triangular configuration)

In the triple motor test, the centerlines of each motor were arranged in a triangle pattern. The heat flux to the side rail was much higher than that seen in the single motor test. Because of this, many of the thin plates used in the lumped mass capacitance method (intrinsic thermocouples) warped and cracked or ruptured. Fortunately, the insulation that wrapped the thermocouples protected the bundle which yielded data from thermocouples further down the rail. The point of rupture for each intrinsic thermocouple was evident from the thermocouple data. Figure 15 summarizes the results of these heat fluxes at the various locations for the triple motor test.

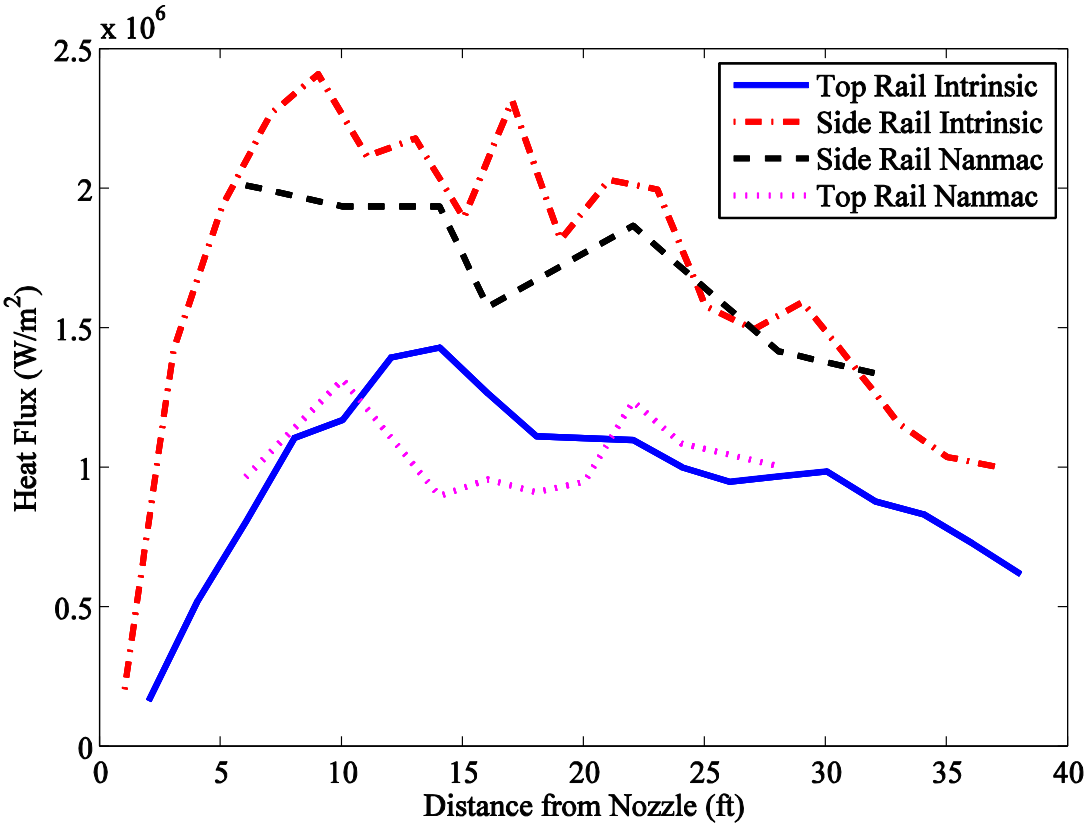

Figure 15. Triple Motor Heat Flux Results with Distance from the Nozzle

The thermocouple plates that did not rupture provided similar data to the thermocouple plates that did rupture prior to becoming compromised. Because the DAQ (Data Acquisition Assistant) is continuously recording, previous data is not compromised when a thermocouple is destroyed. Therefore, even though some of the intrinsic thermocouples were destroyed, heat flux data can still be graphed using the data prior to rupture.

In general, most of the rail locations agree that the maximum temperature seen in the plume is located around 10 ft. past the nozzle. This is because the propellant used in this experiment expels unburned hydrogen which ignites when exposed to air. This does not occur at the nozzle because air needs to entrain with the propellant plume and reach the rich flammability limit for a gaseous mixture with hydrogen. This reaction takes place close to the surface of the rope (or instrument rail) and provides a high heat flux in addition to the radiation from the rest of the plume. A maximum temperature seen at the rail is expected somewhere downstream of the nozzle. In the single motor test, a maximum of about 1.2 MW/m^2 was observed with the NANMAC® thermocouples. In the triple motor test, a maximum heat flux of about 2 MW/m^2 was observed in the side rail.

3.4.Full-Scale Tests (Triple motor arranged in linear configuration and comparison to single motor)

In addition, heat flux was measured from three motors side by side, i.e., linear arrangement, and compared to the heat flux from a single motor. These two measurements were made at the same distance from the plume. For this arrangement, no additional heat flux could be seen by the top rail in the three motor test. Based on the results from the experiment, the plume radiates near that of a blackbody, and very little (if any) additional heat flux was seen in the three axial motors

test as seen in Figure 16. Consequently, the plume in the single motor test is indicated to be optically thick.

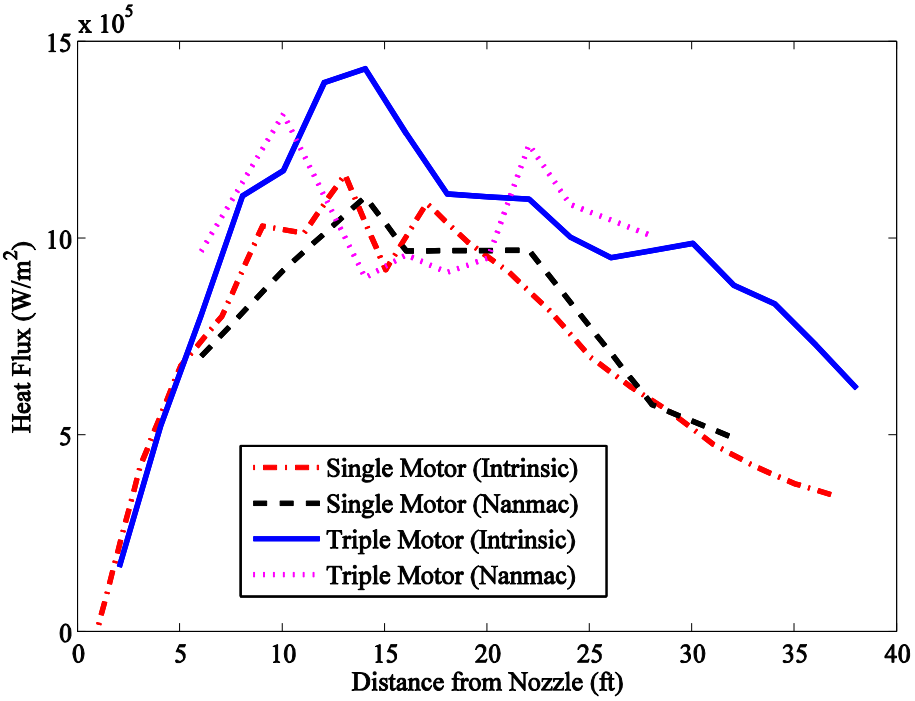

Figure 16. Comparison of Top Rail in the Triple Motor Test (linear arrangement) to the Side Rail for the Single Motor Test

When the NANMAC® results are compared against one another, there is no appreciable difference between heat flux in the three motor test and the heat flux in the single motor test (considering uncertainty in measurement). When the intrinsic results are similarly compared, the heat flux in the three motor test was approximately 1.2 times that of the single motor (however, the uncertainty in these measurements are likely above 20%). Therefore, it is possible to conclude that the heat flux seen by the rope from 14 motors (which is the number of motors anticipated in normal usage) will not be above 1.2 times the heat flux seen in the 3 motor test. The three motor test viewed from the side, yielded heat fluxes of approximately 2 MW/m^2 as seen in Figure 14.

Based on these results, the thermocouple response of the rope in the triple motor test can be taken as the approximate temperature the plasma rope will experience in a full scale test. Since the temperatures were well within the 573K limitation for the rope, and the insulation was intact post-test, it is reasonable to conclude that the plasma rope will not fail under these conditions for a full 14-motor experiment.

4. Rationalization of Results

While this test series had a specific objective, i.e., to project the survival of an insulated tow rope to heat flux in the proximity of the plume from a firing rocket motor, some generalizations can be suggested so that these results can perhaps be applied to other, similar needs.

- Until the plume contacts the gage, radiation is the dominating heat transfer mode.
- When the cone from the firing motor contacts the heat flux gauge at 15 ft., a peak is seen, presumably due to the combined effect of convection and radiation with a high view factor.
- Air entrainment and plume cooling at greater distances causes a reduction from the maximum heat flux.
- Solid rocket propellant plumes appear to be optically thick even in the case of small motors. This observation will of course be influenced by solid components in the plume, such as aluminum particles, or alumina smoke.

5. Conclusion

The thermocouples performed better than anticipated and yielded heat flux results extremely close to those from model calculations. Based on these results, heat fluxes were inferred for each thermocouple location along the rail for both the single and triple motor tests. From the rope

response to the triple motor test, and the assumption that a single motor plume is relatively optically thick, the rope should survive the full scale 14 motor test.

Acknowledgments

Sandia National Laboratories is a multi-program laboratory managed and operated by Sandia Corporation, a wholly owned subsidiary of Lockheed Martin Corporation, for the U.S. Department of Energy's National Nuclear Security Administration under contract DE-AC04-94AL85000.

References

[1] Hunter, L. W., et al., 2007, "The Environment Created by an Open-Air Solid Rocket Propellant Fire". *Combustion Science and Technology*, 179, pp. 1003-1027.

[2] Lee, D. O., Hardee, H. C., and Donaldson, A. B., 1975, "Thermal Model for Solid Propellant Fires", Sandia National Laboratories, SAND75-0051.

[3] Nicolette, V. F., and Hewson, J. C., *Solid Propellant Fire Modeling in Support of the Mars Science Laboratory Mission, JANNAF 2008,* Boston, MA (May 2008)

[4] Height, J. L., Donaldson, A. B., Gill, W., Parigger, C. G., "Measurements in Solid Propellant Plumes at Ambient Conditions*", IMECE2011-62726, Proceedings of the ASME International Mechanical Engineering Conference and Exposition*, November 11-17, 2011, Denver, CO.